Comparative Study of Radionuclide Uptake Levels between Primary and Metastatic Bone Tumors

Yigbedeck Yolande Ebele Huguette[1], Kyere Augustine Kwame[1], Wilson Isaac Kojo[2], Hasford Francis[1,3], Sosu Edem Kwabla[1,3], Ankrah Alfred Otoe[2]

[1]Department of Medical Physics, School of Nuclear and Allied Sciences, University of Ghana, [2]Department of Nuclear Medicine, National Centre for Radiotherapy and Nuclear Medicine, Korle-Bu Teaching Hospital, [3]Medical Radiation Physics Centre, Radiological and Medical Sciences Research Institute, Ghana Atomic Energy Commission, Accra, Ghana

Abstract

Study on 95 patients to compare radionuclide uptake levels in patients undergoing bone scintigraphy at a Nuclear Medicine Unit has been performed quantitatively using Image J software. Patients were administered with activity ranging from 0.555 to 1.110 MBq depending on their body weight, and their whole-body bone scans obtained with an installed e.cam single-photon emission computed tomography system. Matrix size of 256×1024 was used in acquiring the scintigrams. Quantitative analyses performed with installed Image J software revealed higher radionuclide uptake levels in metastatic tumors compared with primary tumors for all selected skeletal parts. Average normalized count of activity in metastatic tumors was 37.117 ± 27.740 cts/mm^2/MBq and its corresponding uptake in primary tumors was 23.035 ± 19.542 cts/mm^2/MBq. The relative higher uptake in metastatic tumors over primary tumors could be attributed to higher osteoblastic activity and blood flow in metastatic tumors.

Keywords: Counts of activity, diagnosis, metastatic tumor, primary tumor, quantitative assessments, radionuclide, scintigraphy, single-photon emission computed tomography, therapeutic

Introduction

A nuclear medicine procedure uses Tc-99m methylene diphosphonate (MDP) for diagnostic evaluation of patients with metastatic and nonmetastatic conditions of the bones.[1,2] Bone scans for diagnosis of skeletal disorders constitute the most popular application of radionuclide imaging. Bone scintigraphy is a valuable tool not only for early diagnosis, but also to localize and quantify muscular involvement in the disease. Furthermore, it is useful in monitoring therapeutic responses.[3-5] Bone scintigraphy is a highly sensitive diagnostic procedure, widely available, and relatively inexpensive method for diagnosing many skeletal disorders. The greatest strength of the radionuclide scan relates to its ability to provide early physiologic information about the involved bone and to evaluate multiple areas in a single, relatively rapid examination. Improved imaging techniques such as single-photon emission computed tomography (SPECT) and three-phase scanning, coupled with quantitative assessments of scintigrams, have improved scintigraphy's diagnostic specificity and accuracy for many bone examinations.[6-8]

Bone scintigraphy is a very sensitive analytical modality, which depends ultimately on the ability of the nuclear medicine physician to interpret the image obtained after scanning the patient. It is in this area that the subjectivity of the physician impacts on the outcome of the patient's diagnosis. Hence, it would be desirable to adopt measures of decreasing as much as possible the physician's subjectivity in the interpretation of the scan. However, some few works have been done by Mettler *et al.*,[9] Jones *et al.*,[10] Thrall *et al.*,[11] Ludwig *et al.*,[12] Subramanian *et al.*,[13] and others on radionuclide bone scintigraphy in nuclear medicine.

Quantitative approaches are being employed to determine the relative differences in levels of radionuclide uptake

Address for correspondence:
Mr. Francis Hasford, Medical Radiation Physics Centre, Radiological and Medical Sciences Research Institute, Ghana Atomic Energy Commission, P.O. Box LG 80, Legon, Accra, Ghana. E-mail: haspee@yahoo.co.uk

between primary and metastatic bone tumors. This calls for the application of credible quantitative assessment tools such as Image J (Wayne Rasband, National Institutes of Health, United States of America)[14] which is freely available and operates on a range of platforms such as Windows, Mac, and Linux for image processing. The approach will in general aid in developing mechanisms that rely not so much on how the physician sees the bone scan, but on the physical evidence provided by data captured in the image.

The application of Image J to the analysis of the uptake will allow for accurate interpretation of bone scintigrams in both primary and metastatic bone tumor conditions. Like other quantitative analytical tools, Image J enhances not only diagnostic value but therapeutic effects in nuclear medicine. In addition to being readily available for no cost on image website, Image J is supported by a wide range of constantly evolving user-created functionalities to address a remarkable range of applications, complementing commercial software that typically comes with imaging instruments. By performing quantitative analysis, better attention is paid to detail, and hence better diagnostic outcomes are produced. The primary objective of this study is to quantitatively assess radionuclide uptake levels in primary and metastatic bone tumors for patients undergoing scintigraphic procedures. The uptake levels are characterized by the number of counts in specific regions of interest (ROI) in the scintigrams.

Materials and Methods

The e.cam single-photon emission computed tomography system

The primary equipment employed in obtaining bone scintigrams for this study was the Siemens e.cam SPECT system (Siemens Medical Solutions Inc, Valley Stream Parkway, USA). The equipment is connected to a computer system, which displays acquired images. Figure 1 shows the process through which images are obtained. The SPECT system is equipped with a low energy all purpose collimator during bone scans.
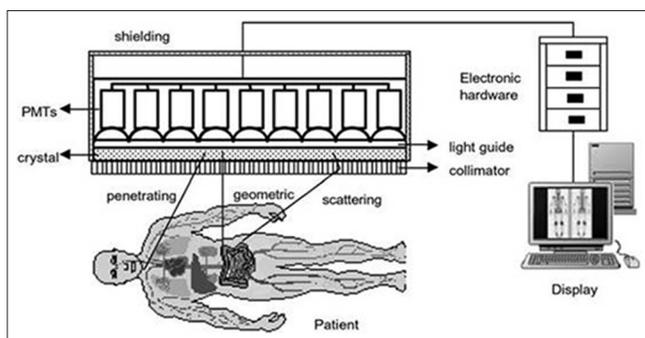

Figure 1: System of image acquisition using e.cam single-photon emission computed tomography system

Acquisition of bone scintigrams

Tc-99m methylene diphosphonate was prepared in the hot laboratory of the Nuclear Medicine Unit and intravenously administered to patients immediately after preparation. Anterior and posterior whole-body planar images were acquired three hours after administration of the radiopharmaceutical. Administered activity typically ranged from 0.555 to 1.110 MBq depending on a patient's weight and age. Patients were made to drink four to six glasses of water between the time of injection and time of image acquisition to aid in rapid clearance of radioisotope from the bladder. A 256 × 1024 matrix size was used in acquiring the bone scintigrams. The acquired images were displayed in grayscale for a resident nuclear medicine physician's interpretation and diagnosis.

Figure 2 displays anterior-posterior views of a patient's scintigram saved in joint photographic experts group format. The scintigrams were retrieved from the database of the Nuclear Medicine Unit and analyzed in terms of radionuclide uptake levels using Image J software.

Image J software

Image J, a comprehensive image quantitative analytical tool, was installed on a Dell Vostro 1014 Laptop (Dell Computers Corporation, Round Rock, Tx, USA) computer. Image J software is a digital imaging program, which displays, edits, analyzes, processes, saves, and prints images. The software also supports standard image processing functions such as contrast manipulation, sharpening, smoothing, edge detection, median filtering and thresholding, histogram generation, and profile plots.[14-16]

Assessment of radionuclide uptake levels

Pathologic whole-body bone scintigrams of 95 patients acquired with the Siemens e.cam SPECT system between 2007 and 2012 were retrieved for this study. For ethical

Figure 2: Whole-body bone scintigram of a patient showing multiple hot spots

reasons, patients were coded with ID numbers instead of their names. Appendix A shows data on patients sampled for this study.

Hot spots on the sampled scintigrams representing pathologic conditions were identified and classed either as primary or metastatic bone tumors by a resident nuclear medicine physician. For the purposes of this study, selection of hot spots were restricted to nine skeletal parts namely cranium, neck, sternum, shoulder, ribcage, vertebra, knee, femur, and sacrum due to their dominance over hot spots recorded in other skeletal parts.

Hot spots in the mandible, hip, and ankle were excluded in the selection criteria. Mandibular hot spots were all diagnosed as dental diseases and not bone pathology. All hot spots in the hip were metastatic in nature, while hot spots in the ankle were all primary in nature, hence comparative assessments of primary and metastatic uptakes in those regions could not be possible.

The sampled scintigrams were imported into Image J software in succession and analyzed by drawing ROI over observable hot spots (tumor sites). Oval selection tool was employed in drawing the ROIs because bone tumors usually have oval or rounded shapes,[17-19] and hence best approximation is achieved with this tool. Counts of activity for selected ROIs were generated in Image J for each patient, and recorded in excel spread sheet for analyses. For each identified tumor site, counts of activity for both anterior and posterior views were generated from Image J, and the geometric mean count (GMC) estimated using eq. (1). The counts of activity (i.e. the GMCs) for the tumor sites were then normalized relative to the respective area of ROI and injected activity. The normalized geometric mean counts (nGMC), which give an indication of the radionuclide uptake level, were estimated using Eq. (2).

$$\text{GMC} = \sqrt{\text{anterior mean counts} \times \text{posterior mean counts}} \quad (1)$$

nGMC (uptake level)

$$= \frac{\text{GMC (cts)}}{\text{area of ROI (mm}^2) \times \text{injected activity (MBq)}} \quad (2)$$

The estimated normalized counts, referred to as radionuclide uptake level in this paper, were grouped into the various skeletal parts and average values calculated as shown in Table 1. Differences in primary and metastatic uptake levels for the nine skeletal parts were analyzed.

Standard deviation or root mean square error estimates were performed using eq. (3).

$$\text{SD} = \sqrt{\frac{\sum (x - \bar{x})^2}{N}} \quad (3)$$

where $\bar{x}$ is the mean of n sampled values.

Result and Discussion

Table 2 shows the uptake levels (nGMCs) for the nine selected body parts. Tumor sites in the studied patients varied in number. Some patients recorded single tumor sites, while others recorded multiple sites. From the 95 studied patients, four (i.e. 042, 045, 067 and 072) recorded single tumor sites in their scintigrams, while five (i.e. 003, 032, 037, 038 and 052) recorded two tumor sites on their scintigrams. The rest of the patients had three or more tumor sites in the body.

Figure 3 indicates the number of patients in each of the nine categories of analyzed skeletal parts. Except for neck, knee and sacrum categories, metastatic tumors dominated over primary tumors in all other categories. A total of 271 tumors from the 95 patients were considered in the analyses, resulting in an average of 2.9 tumors per patient. For the studied population, bone tumors detected in the shoulder region was the most dominant with 23.6% and tumors in the sacrum were least with 1.5%. Metastatic tumors made up 64.6% of all detected bone tumors, while primary tumors made up 35.4%. This observation corroborates similar observation by Hasford *et al.*[20] that bone tumors with

Table 1: Percentage difference between metastatic and primary uptake

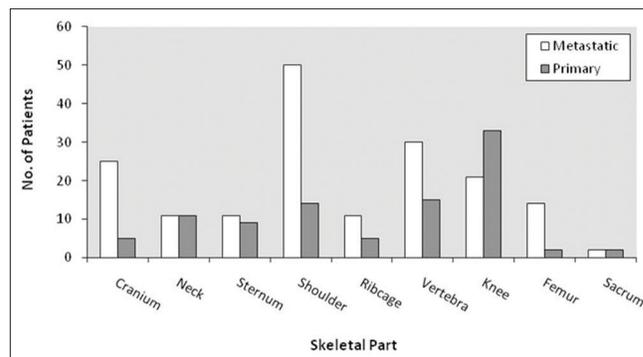| Skeletal part	Normalized counts of activity nGMC (cts/mm²/MBq)		Percentage difference
	Metastatic	**Primary**	
Cranium	10.608	5.276	50.3
Neck	68.360	31.909	53.3
Sternum	19.209	10.007	47.9
Shoulder	25.004	18.811	24.8
Ribcage	97.555	72.757	25.4
Vertebra	52.846	29.692	43.8
Knee	17.443	11.868	32.0
Femur	23.153	17.510	24.4
Sacrum	19.874	9.484	52.3
Average	37.117	23.035	37.9

nGMC: Normalized geometric mean count

Figure 3: Number of patients in the respective bone tumour categories

Table 2: Average normalized uptakes for the selected body parts

Skeletal part	Metastatic				Primary			
	No. of patients	nGMC (cts/mm^2/MBq)	Error		No. of patients	nGMC (cts/mm^2/MBq)	Error	
			$(x-\bar{x})$	$(x-\bar{x})^2$			$(x-\bar{x})$	$(x-\bar{x})^2$
Cranium	25	10.608	−26.509	702.727	5	5.276	−17.759	315.382
Neck	11	68.360	31.243	976.125	11	31.909	8.874	78.748
Sternum	11	19.209	−17.908	320.696	9	10.007	−13.028	169.729
Shoulder	50	25.004	−12.113	146.725	14	18.811	−4.224	17.842
Ribcage	11	97.555	60.438	3652.752	5	72.757	49.722	2472.277
Vertebra	30	52.846	15.729	247.401	15	29.692	6.657	44.316
Knee	21	17.443	−19.674	387.066	33	11.868	−11.167	124.702
Femur	14	23.153	−13.964	194.993	2	17.510	−5.525	30.526
Sacrum	2	19.874	−17.243	297.321	2	9.484	−13.551	183.630
		Average nGMC: $\bar{x}=37.117$	SD=27.740			Average nGMC: $\bar{x}=23.035$	SD=19.542	

nGMC: Normalized geometric mean count; SD: Standard deviation

their origin in cells of the bone itself are less prevalent compared with those that metastasize from other parts of the body.

Counts of activity

Table 2 summarizes the counts of activity for the selected body parts. The normalized counts of activity in the metastatic and primary tumors were 37.117 ± 27.740 cts/mm^2/MBq and 23.035 ± 19.542 cts/mm^2/MBq, respectively for the entire patient population.

All nine skeletal parts considered in the study show high counts of activity in metastatic tumors compared to the primary tumors. The higher a radionuclide uptake level, the higher its corresponding count of activity and vice versa. Hence from results of the study, metastatic bone tumors are seen to have higher radionuclide uptake level compared with primary bone tumours [Figure 4]. This observation could be attributed to the mechanism of Tc-99m MDP uptake, which is directly related to blood flow and degree of osteoblastic activity. Bony metastatic disease results in carcinomatous osteodysplasia, referring to histologic alteration, resulting in a variable increase in osteoblasts, osteoclasts, blood vessels, and other stromal tissues.[21] The resultant effect is an increased activity in a bone scan.

Difference in uptake levels

The percentage differences between counts of activity in metastatic and primary bone tumors are estimated in Table 1. Highest percentage difference is observed in the neck with 53.3% and the least difference in the femur with 24.4%. The radionuclide uptake level in the metastatic tumors was estimated to be 37.9% more than uptake in the primary tumors in the entire patient population. The study has proved a significantly higher uptake of Tc-99m MDP in metastatic cases than in primary cases using a quantitative approach.
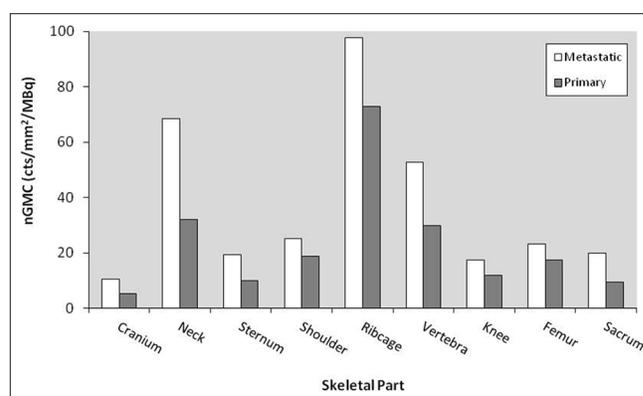

Figure 4: Normalized counts of activity in the studied patient population

Conclusion

Comparative assessment of radionuclide uptake levels has been performed using Image J software on patient scintigrams. The study has revealed higher uptake of activity in metastatic bone tumors compared with primary tumors. The higher uptakes in metastatic cases have been attributed to the mechanism of Tc-MDP uptake, which is directly related to blood flow and degree of osteoblastic activity. Quantitative assessment of bone scintigrams is recommended due to its relatively high accuracy in diagnosing tumors.

Acknowledgement

References

1. O'Reilly PH, Shields RA, Testa HJ. Nuclear Medicine in Urology and Nephrology. 2nd ed. London: Butterworths and Co.; 2000. p. 2-4, 233-4.

2. Zaidi H. Quantitative Analysis in Nuclear Medicine Imaging. New York, USA: Springer; 2006.

3. Otsuka N1, Fukunaga M, Ono S, Nagai K, Morita K, Tomomitsu T, *et al.* Visualization of soft tissue by technetium-99m MDP in polymyositis. Case reports. Clin Nucl Med 1988;13:291-3.

4. Lim ST, Sohn MH, Park SA. Tc-99m MDP three-phase bone scintigraphy in disciplinary exercise-induced rhabdomyolysis. Clin Nucl Med 2000;25:558-9.

5. Bar-Sever Z, Mukamel M, Harel L, Hardoff R. Scintigraphic evaluation of calcinosis in juvenile dermatomyositis with Tc-99m MDP. Clin Nucl Med 2000;25:1013-6.

6. Lurye DR, Castronovo FP Jr, Potsaid MS. Improved method for quantitative bone scanning. J Nucl Med 1977;18:1069-73.

7. Bombardieri E, Aktolun C, Baum RP, Bishof-Delaloye A, Buscombe J, Chatal JF, *et al.* Bone scintigraphy procedure guidelines for tumour imaging, September 2, 2003. Available from: http://www.eanm.org/publications/guidelines/gl_onco_bone.pdf. [Last accessed on 2013 Aug 05].

8. McNeil BJ. Rationale for the use of bone scans in selected metastatic and primary bone tumors. Semin Nucl Med 1978;8:336-45.

9. Mettler FA Jr, Guiberteau MJ. Nuclear Medicine Imaging. 3rd ed. Philadelphia, USA: W. B. Saunders Company 1998. p. 207-11.

10. Jones AG, Francis MD, Davis MA. Bone scanning: Radionuclide reaction mechanisms. Semin Nucl Med 1978;8:336-45.

11. Thrall JH, Geslien GE, Corcoron RJ, Johnson MC. Abnormal radionuclide deposition patterns adjacent to focal skeletal lesions. Radiology 1975;115:659-63.

12. Ludwig H, Kumpan W, Sinzinger H. Radiography and bone scintigraphy in multiple myeloma: a comparative analysis. Br J Radiol 1982;55:173-81.

13. Subramanian G, McAfee JG, Blair RJ, Kallfelz FA, Thomas FD. Technetium-99m-methylene diphosphonate – A superior agent for skeletal imaging: comparison with other technetium complexes. J Nucl Med 1975;16:744-55.

14. Collins TJ. ImageJ for microscopy. Biotechniques 2007;43 1 Suppl: 25-30.

15. Burger W, Burge M. Digital Image Processing: An Algorithmic Approach Using Java. New York, USA: Springer; 2007.

16. Dougherty G. Digital Image Processing for Medical Applications. New York, USA: Cambridge University Press; 2009.

17. Ghasemi A, Hiradfar AA, Pedram M. An epidemiologic study of ewing sarcoma family at SHAFA Hospital in Khozestan Province-IRAN, a referral children cancer treatment center. Iran J Ped Hematol Oncol 2012;1:24-6.

18. Kemal B, Haydar D, Şule C, Övgü A, Gülben EH, Meltem O, *et al.* Giant cell tumour-like lesion of the urinary bladder: A report of two cases and literature review; giant cell tumour or undifferentiated carcinoma? Diagn Pathol 2009;4:48.

19. Li S, Siegal GP. Small cell tumors of bone. Adv Anat Pathol 2010;17:1-11.

20. Hasford F, Amuasi JH, Sosu EK, Nani K, Sackey TA, Boadu M, *et al.* Radionuclide Tc-99m MDP imaging for diagnosis of bone tumours at Korle-Bu Teaching Hospital (Ghana) – An illustrative review. J Appl Sci Technol 2010;15:1-15.

21. Bader DA, Nagel JS. Bone scintigraphy in multiple myeloma, 1995. Available from: http://www.med.harvard.edu/JPNM/TF94_95/Jan17/WriteUpJan17.html. [Last accessed on 2013 May 13, 06:10:31 GMT].

Appendix

Appendix A: Bio data, clinical history, injected activity of sampled patients

Patient ID	Age (years)	Gender	Clinical history	Injected activity (MBq)
001	67	M	Ca prostate	0.929
002	67	M	Ca prostate	0.810
003	54	F	Ca breast	0.704
004	80	M	Ca prostate	0.770
005	52	F	Ca breast	0.951
006	61	M	Ca prostate	0.858
007	77	M	Ca prostate	0.777
008	65	F	Ca breast	0.814
009	64	M	Ca prostate	0.895
010	76	F	Ca breast	0.803
011	65	M	Ca prostate	0.814
012	28	F	Ca breast	0.818
013	68	M	Ca prostate	0.685
014	70	M	Ca prostate	0.833
015	72	M	Ca prostate	0.910
016	62	M	Ca prostate	0.773
017	30	M	Ca prostate	0.673
018	84	M	Ca prostate	0.673
019	81	M	Ca prostate	0.777
020	71	F	Ca breast	0.803

Contd...

Appendix A: Continued

Patient ID	Age (years)	Gender	Clinical history	Injected activity (MBq)
021	74	M	Ca prostate	0.655
022	54	M	Ca prostate	0.673
023	69	M	Ca prostate	0.633
024	61	M	Ca larynx	0.611
025	74	M	Ca prostate	0.503
026	74	M	Ca prostate	0.481
027	72	M	Ca prostate	0.640
028	69	F	Ca breast	0.577
029	69	M	Ca prostate	0.525
030	70	F	Ca breast	0.524
031	73	M	Ca prostate	0.525
032	75	M	Ca prostate	0.574
033	67	M	Ca prostate	0.740
034	53	F	Ca breast	0.814
035	74	M	Ca prostate	0.566
036	70	M	Ca prostate	0.585
037	67	M	Ca prostate	0.607
038	88	M	Ca prostate	0.618
039	75	M	Ca prostate	0.577
040	82	M	Ca prostate	0.440
041	74	M	Ca prostate	0.677

Contd...

Appendix A: Continued

Patient ID	Age (years)	Gender	Clinical history	Injected activity (MBq)
042	68	M	Osteosarcoma	0.773
043	57	F	Ca breast	0.719
044	51	F	Ca breast	0.688
045	62	F	Spine metastasis?	0.740
046	75	F	Cervical pain	0.703
047	54	M	Ca prostate	0.788
048	69	M	Ca prostate	0.718
049	67	F	Ca breast	0.770
050	73	M	Ca prostate	0.492
051	55	F	Ca breast	0.951
052	49	M	Ca prostate	1.136
053	63	M	Ca prostate	0.825
054	27	F	Ca breast	0.592
055	58	M	Ca prostate	0.585
056	69	M	Ca prostate	0.614
057	46	F	Ca breast	0.433
058	69	F	Ca left lung	0.463
059	71	M	Ca prostate	0.451
060	79	M	Ca prostate	0.511
061	86	M	Ca prostate	0.451
062	61	M	Bone metastasis	0.585
063	34	F	Ca breast	0.648
064	41	F	Ca right breast	0.444
065	72	M	Ca prostate	0.507
066	61	M	Ca lesion	0.740
067	69	M	Ca prostate	0.784
068	48	F	Ca breast	0.518

Contd...

Appendix A: Continued

Patient ID	Age (years)	Gender	Clinical history	Injected activity (MBq)
069	63	F	Ca breast	0.592
070	61	M	Ca prostate	0.500
071	82	M	Ca prostate	0.710
072	71	M	Ca prostate	0.607
073	49	F	Ca breast	0.784
074	43	F	Ca breast	0.444
075	71	M	Ca prostate	0.662
076	31	F	Ca breast	0.503
077	80	M	Ca prostate	0.396
078	72	M	Ca prostate	0.877
079	50	M	Ca prostate	0.977
080	85	M	Ca prostate	0.740
081	69	M	Ca prostate	0.581
082	65	M	Ca prostate	0.692
083	65	M	Ca prostate	0.655
084	22	M	Ca prostate	0.537
085	72	M	Ca prostate	0.636
086	85	M	Adenocarcinoma	0.681
087	68	M	Ca prostate	0.796
088	69	M	Ca prostate	0.581
089	78	M	Ca prostate	0.507
090	79	M	Ca prostate	0.500
091	61	M	Ca prostate	0.418
092	41	M	Ca prostate	1.110
093	61	M	Ca prostate	1.006
094	40	F	Ca breast	1.103
095	64	M	Ca prostate	1.173

Ca: Cancer; M: Male; F: Female